日本雪氷学会誌 雪氷
72巻6号（2010年11月）377－390頁

論 文

Road surface temperature model accounting for the effects of surrounding environment

Naoto TAKAHASHI[1)], Roberto A. TOKUNAGA[1)], Takamitsu SATO[2)] and Nobuyoshi ISHIKAWA[3)]

Abstract

To facilitate proper snow and ice control operations, it is essential to identify and forecast road surface temperature (RST) and/or road conditions. Our research group has directed efforts towards developing a RST model by utilizing a heat balance method that can account for the effects of vehicular traffic. The basic model closely reproduces the RST variation, but it tends to underestimate RST relative to measured RST. We thought this underestimation might be due to not considering the effect of structures along the roadway, and we developed a revised model that incorporates the shielding effect of roadside structures and long-wave radiation (LWR) emission from such structures. The revised model's validity was examined by onsite measurement of LWR. The LWR estimated by the revised model showed a root mean square error (RMSE) of 17.8 W m^{-2}. The RMSE of RST estimated by the revised model was 1.9 degrees Celsius for the whole day, 2.4 degrees Celsius in the daytime and 1.3 degrees Celsius in the nighttime. This is an improvement in RMSE from the basic model by 1.6 degrees Celsius for the whole day, 1.5 degrees Celsius in the daytime, and 1.7 degrees Celsius in the nighttime for the whole period analyzed.

Key words: road surface temperature, heat balance method, roadside structures, long-wave radiation
キーワード：路面温度，熱収支法，沿道構造物，長波放射

1. Introduction

Accurate forecasting of winter road conditions, whether the road surface is icy or not, is essential to facilitate proper snow and ice control operations. Hokkaido has a cold, extremely snowy climate. Sapporo, Hokkaido's central city, has an annual snowfall of 6 meters, and the average daily temperature from December to February is below 0 degrees Celsius. With a population of 1.9 million, the city is one of the few of its size in the world with such severe snow conditions. The city also has heavily trafficked routes with over 40000 vehicles per day, and about half of the highway network runs alongside buildings.

To perform snow and ice control operations for roads appropriately in such an urban situation, a road surface temperature (RST) model must be developed that considers the influence of running vehicles and roadway structures.

This study takes the approach of revising the basic model of Takahashi *et al.* (2006) by

1) Civil Engineering Research Institute for Cold Region, 1–3 Hiragishi, Toyohira-ku, Sapporo, 062–8602, Japan
2) Japan Weather Association, 3–1–1 Higashi-Ikebukuro, Toshima-ku, Tokyo, 170–6055, Japan
3) Institute of Low Temperature Science, Hokkaido University, Kita-19 Nishi-8, Kita-ku, Sapporo, 060–0819, Japan

factoring in the effect of structures along the roadway. Long-wave radiation (LWR) was monitored at the study point for the purpose of improving the predicted accuracy during hours without sunlight, and the accuracy of the model was verified.

2. Literature review

Numerous RST models have been developed and utilized by road and traffic engineers around the world. These models can be generally categorized into two approaches: statistical modeling and heat-balance modeling. Mahoney and Wagoner (2005) reported that the majority of the models used operationally are heat-balance models that calculate RST.

Among early heat-balance models, Rayer (1987) developed one with meteorological factors as parameters. Various such models have been examined and developed, but there is no simple way of evaluating the models in terms of performance.

For instance, Thornes and Shao (1991) tested a RST model's sensitivity of individual meteorological parameters, e.g., air temperature, cloud cover and type, solar radiation and wind speed, and found that air temperature was the most influential parameter controlling RST. Brown and Murphy (1996) indicated that prediction performance was improved by combining the RST models formulated by two organizations: the UK Meteorological Office and Oceanroutes. In contrast, Shao and Lister (1996) developed a fully automated RST model that requires no external meteorological input data other than automatically collected sensor measurements of surface temperature, air temperature, dew point and wind speed from the forecast site.

In Japan, statistical RST models have been developed to a practical level (Civil Engineering Research Institute, 2005). In addition, a heat-balance model with meteorological factors as its parameters was recently developed (Seki *et al.,* 2006).

For more accurate prediction, the above authors indicate that models should include accurate road characteristic data, in addition to weather data. As road characteristic data, Takle and Hansen (1990) and Bentz and Dale (2000) developed a heat-balance model that focuses on road structures to predict bridge surface conditions.

Also, Ishikawa *et al.* (1999) and Prusa *et al.* (2002) indicated that running vehicles affect RST, and Takahashi *et al.* (2006) developed a heat-balance model that considers the influence of running vehicles. This model considers the shielding effect of vehicles, as well as the LWR they emit. However, the model shows a large error, especially at night. This might be from the influence on LWR of structures along the roadway and from elevated roadways is not considered. Indeed, some models consider heat from vehicles as well as the blocking of LWR from the atmosphere (Prusa *et al.,* 2002 ; Chapman and Thornes, 2005).

Furthermore, Johnson *et al.* (1991) identified the effect of shielding by and LWR from buildings along roadways, by measuring long-wave radiant quantities in urban and rural areas. Another unique finding was made by Chapman *et al.* (2001). They examined the meteorological and geographical parameters that influence RST, and they found that sky-view factors control surface temperatures under conditions of high atmospheric stability.

In urban areas, it is particularly necessary to consider the effects of environmental factors such as traffic and buildings. Indeed, Narita (2001) pointed out that downward long-wave flux from surrounding buildings and structures should be included in net atmospheric radiation. However, there are no RST models that have introduced and formulized the impact of both running vehicles and surrounding

buildings.

3. Model development

3.1 Outline of the basic model

This study takes the approach of developing a model that considers the effects of structures along roadway, based on the model of Takahashi *et al.* (2006). This section explains the heat balance model developed by Takahashi *et al.* (2006), which considers the influence of running vehicles (hereinafter: "the basic model").

Figure 1 shows a conceptual diagram of the basic model. The vehicle-related factors influencing RST include atmospheric and solar radiations, which are screened by vehicles, and infrared radiation, which is emitted by the bodies of vehicles. These factors vary by traffic volume. The energy input into the road surface includes infrared radiation, sensible heat flux, latent heat flux, and ground heat flux from the road surface. RST can be determined from the heat transfer through the surface. This is a major component of the heat-balance, and it is expressed by Equations (1) and (2). This model was developed under the assumption of an asphalt road surface on an urban arterial highway with a high level of management.

$$R^{\downarrow}=\varepsilon_r\sigma T_s^4+H+lE+G \tag{1}$$

where

$R^{\downarrow}$ = radiant input quantity,
ε_r = emissivity of the outgoing LWR from road surface,
σ = Stefan-Boltzman constant,
T_s = RST,
H = sensible heat flux,
lE = latent heat flux, and
G = ground heat flux.

$$R^{\downarrow}=(1-\alpha)S_r^{\downarrow}+L_r^{\downarrow}+L_c \tag{2}$$

where

$S_r^{\downarrow}$ = global solar radiation,
α = reflectivity (albedo),
$L_r^{\downarrow}$ = atmospheric radiation into the road surface, and
L_c = infrared radiation into the road surface from vehicular traffic.

The parameters applied in Equation (1) are presented in Equations (3) to (5).

$$H=C_p\rho C_h U(T_s-T_a) \tag{3},$$

$$lE=\rho\frac{0.622l}{P}C_e U\beta(e_{ss}-e_a) \tag{4},$$

$$G=\kappa\frac{T_s-T_g}{\Delta z} \tag{5}.$$

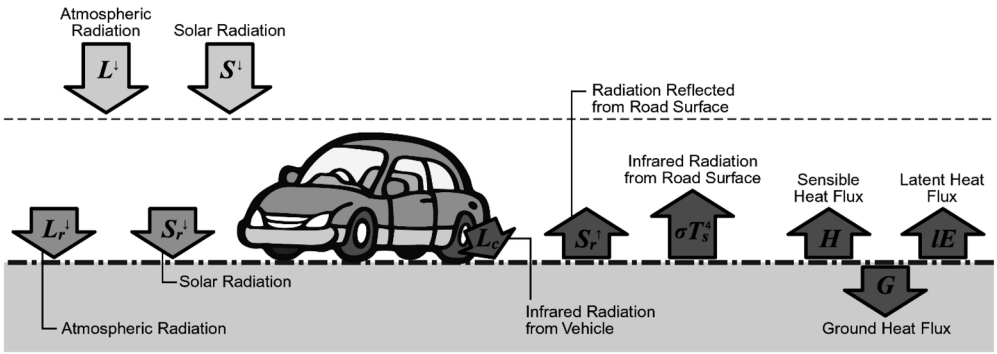

Fig. 1 Conceptual diagram of heat transfer at the road surface.

where

C_p = specific heat capacity of air,
ρ = density of air,
C_h = turbulent diffusion coefficient in sensible heat flux (bulk coefficient)
U = wind velocity,
T_a = air temperature,
l = latent heat of vaporization,
P = atmospheric pressure,
C_e = turbulent diffusion coefficient in latent heat flux (bulk coefficient)
β = evaporation efficiency,
e_{ss} = surface saturation vapor pressure,
e_a = atmospheric vapor pressure,
κ = thermal conductivity,
T_g = subsurface temperature at depth Δz, and
Δz = depth at which T_g is measured

Here each parameter in Equation (2) is explained. When vehicles travel on the road, the surface absorbs only scattered radiation; when no vehicles travel on the road, the surface absorbs both scattered and direct solar radiation. Therefore, $S_r{}^{\downarrow}$ is presented in Equation (6).

$$S_r{}^{\downarrow} = (1-t_r)S^{\downarrow} + t_r S_s{}^{\downarrow} \quad (6)$$

where

t_r = ratio of time that vehicles are on the road,
$S^{\downarrow}$ = solar radiation in open skies, and
$S_s{}^{\downarrow}$ = scattered radiation.

Then, the ratio of time that vehicles are on the road (t_r) is presented in Equation (7).

$$t_r = \frac{d \cdot N}{v} \quad (7),$$

where

d = average vehicle length,
N = traffic volume, and
v = average vehicle speed.

$S_s{}^{\downarrow}$ is presented in Equation (8).

$$S_s{}^{\downarrow} = \chi S^{\downarrow} \quad (8)$$

χ shows the ratio of scattered radiation (the ratio of scattered radiation to solar radiation in open skies). Oke (1978) and Erbs *et al.* (1982) demonstrate in their studies that it is between 0.15 and 0.25 at the time of clear sky. At the time of clouded sky, the amount of global solar radiation is small although χ is large and the value of sky solar radiation is small; therefore, it is simply referred to as $\chi = 0.1$.

When vehicles travel on the road, the road surface receives infrared radiation from the underside of the vehicle; when no vehicles are on the road, it receives atmospheric radiation from the sky. Accordingly, $L_r{}^{\downarrow}$ is presented in Equation (9).

$$L_r{}^{\downarrow} = (1-t_r)L_a{}^{\downarrow} \quad (9),$$

where $L_a{}^{\downarrow}$ is atmospheric radiation under the open sky, and $L_a{}^{\downarrow}$ is determined by Kondo's equation (1994). Kondo's equation determines long-wave radiant quantities from the amount of clouds in all sky layers and in lower sky layers. In addition, in the basic model, the shielding effect of any structures along the route is not taken into consideration. L_c is presented in Equation (10).

$$L_c = t_r \varepsilon_v \sigma T_v{}^4 \quad (10),$$

where

ε_v = emissivity of LWR emitted from the vehicle underside,
σ = Stephan- Boltzman coefficient, and
T_v = temperature of the vehicle underside.

The temperature of the vehicle underside var-

Table 1 Parameters needed for calculation.

Heat Balance Composition	Parameter	Unit	Value
Infrared Radiation from Road Surface $\varepsilon_r T_s^4$	Emissivity of the Outgoing LWR from Road Surface ε_r	-	1.0
	Stefan-Boltzman Constant σ	$W\ m^{-2}\ K^{-4}$	5.67×10^{-8}
Sensible Heat Flux H	Specific Heat Capacity of Air C_p	$J\ kg^{-1}\ K^{-1}$	1005
	Density of Air ρ	$kg\ m^{-3}$	1.29
	Bulk Coefficient C_h	-	0.003
Latent Heat Flux lE	Latent Heat of Vaporization l	$J\ kg^{-1}$	2.5×10^{6}
	Atmospheric Pressure P	hPa	1000
	Bulk Coefficient C_e	-	0.003
	Evaporation Efficiency β	-	0.2
Ground Heat Flux G	Thermal Conductivity κ	$W\ m^{-1}\ K^{-1}$	2.1
	Depth Δz	m	0.05
Solar Radiation $S_r{}^{\downarrow}$	Albedo α	-	0.1
	Average Vehicle Length d	m	5
	Average Vehicle Speed v	$km\ h^{-1}$	Intersection: 5 Non-Intersection: 30
	Ratio of Scatted Radiation χ	-	0.1
Infrared Radiation from Vehicle $L_c{}^{\downarrow}$	Emissivity of LWR Emitted from the Vehicle Underside ε_v	-	1.0
	Temperature of the Vehicle Underside T_v	℃	$T_v = T_a$ (air temp.)

ies by location on the vehicle (Watanabe *et al.*, 2005). Thus, in this study, it is referred to as $T_v = T_a$ based on the measurements and study results of Watanabe *et al.* (2005), where T_a is air temperature.

In the basic model, the data necessary for calculation are the time-variable data, including the amounts of solar radiant quantities, air temperature, wind velocity, relative humidity and cloud amount (in all sky layers and in lower sky layers), and the traffic volume. Other parameters use the fixed values shown in Table 1.

3.2 Model improvement

The basic model was revised to more accurately estimate the solar and atmospheric radiation, and expanded to encompass the effect of structures along the roadway. Structures along the roadway have two effects: They block solar and atmospheric radiation and emit LWR. To express these effects mathematically, the rate of radiation shielding, ϕ (the ratio of sky which is blocked by structures along the roadway), was introduced. Taking into account the LWR from surrounding buildings, atmospheric radiation ($L_a{}^{\downarrow}$) is presented in Equation (11).

$$L_{a,\,env}{}^{\downarrow} = (1-\phi)L_r{}^{\downarrow} + \phi L_{strc}{}^{\downarrow} \quad (11),$$

where

$L_{a,\,env}{}^{\downarrow}$ = atmospheric radiation coming from the sky taking into account the roadside environment,

ϕ = rate of radiation shielding, and

$L_{strc}{}^{\downarrow}$ = LWR emitted by structures.

If Equation (11) is substituted for $L_a{}^{\downarrow}$ in Equation (9), the atmospheric radiation, $L_r{}^{\downarrow}$ can be rewritten as,

$$L_r^{\downarrow} = (1-t_r)\{(1-\phi)L_a^{\downarrow} + \phi L_{strc}^{\downarrow}\} \quad (12),$$

and $L_{strc}^{\downarrow}$ is expressed in Equation (13).

$$L_{strc}^{\downarrow} = \varepsilon_{strc}\sigma T_{strc}^{4} \quad (13),$$

where

T_{strc} = surface temperature of structures along the roadway (T_{strc} is assumed here to be equal to T_a), and

ε_{strc} = emissivity of the outgoing LWR from the surface of structures along the roadway.

For solar radiation, we consider the impact of structures along the roadway. Solar radiation entering the road surface at the time of clear sky will be influenced by those structures. The impact of structures on diffuse (scattered) solar radiation is small, and it can be written as Equation (14).

$$S_{env}^{\downarrow} = (1-\phi)S_d^{\downarrow} + S_S \quad (14)$$

where

$S_{env}^{\downarrow}$ = solar radiation taking into account the roadside environment and

$S_d^{\downarrow}$ = direct solar radiation

Substituting Equation (14) for $S^{\downarrow}$ in Equation (6) gives us

$$S_r^{\downarrow} = (1-t_r)(1-\phi)S_d^{\downarrow} + S_s^{\downarrow} \quad (15).$$

In this study, the component of direct solar radiation is presented in Equation (16).

$$S_d^{\downarrow} = (1-\chi)S^{\downarrow} \quad (16)$$

Data necessary for calculation of the revised model are the same as those for the basic model shown in Table 1, except ϕ.

4. Case study outline

4.1 Study point and meteorological observation

A case study was conducted in the winter of 2005–2006 to determine the accuracy improvements of the revised model and to collect meteorological and RST data. The study point selected was along National Route 5 in the northwest suburbs of Sapporo (Fig. 2). The route is an arterial highway crossing Sapporo east-west along which there are many buildings and above which there is an elevated expressway. Such a setting is typical of roadways in urban areas.

RST for verification was acquired from a thermocouple installed at a depth of 5 mm from the road surface. For meteorological data necessary for driving the models, air temperature and wind velocity were observed at the study point. A thermometer and anemometer were installed 3 meters above the road surface so that the sensors would not be disturbed by roadside snow accumulation, nor would they hinder snow removal.

Solar radiation, relative humidity and cloud cover were obtained from the Sapporo District Meteorological Observatory, which is about 5

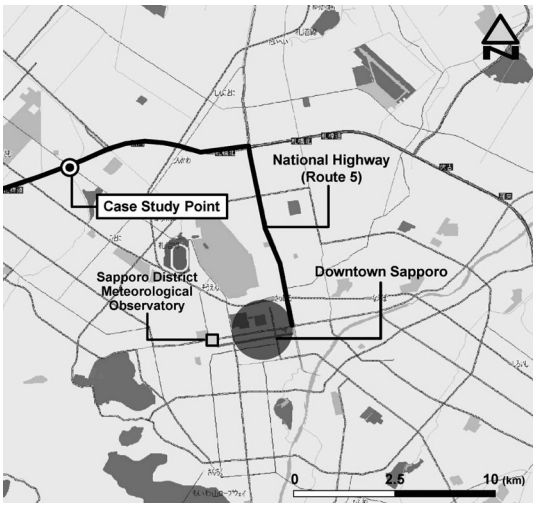

Fig. 2 The case study point.

km from the study point (Fig. 2).

As for the vehicle factor, hourly traffic volume was determined by directly counting the number of vehicles passing through the study point. Also, the study employs the results of traffic analyses conducted by the road authority for v.

4.2 Measuring long-wave radiation and rate of radiation shielding (ϕ)

The rate of radiation shielding (ϕ) by the structures along roadway was calculated by taking a picture of the sky using a camera with a fisheye lens (Fig. 3). Incoming LWR was measured by installing a long- and short-wave radiation sensor (EKO Instruments Co., Ltd.; MR-40; sensitivity: 5μV W^{-1} m^{-2}) at the study point. LWR was collected for the 45 days from January 25 to March 10, 2006. The sensors were installed 3 meters above the road surface so that they would not hinder snow removal. Inspection was carried out once per week during the observation period, which prevented the sensor from being covered by snow.

Fig. 3 Full-sky image of the case study point.

5. Case study results

5.1 Accuracy of modeled long-wave radiation

The accuracy of LWR estimated by the models affects the RST. Figure 4(a) shows the measured LWR and those calculated by the basic model (Equation (9)) and the revised model (Equation (12)) from February 1 to 15, 2006. Figure 4(b) shows the amount of total clouds and lower clouds, which are necessary for calculating the LWR using Kondo's equation. Figure 4(c) shows the atmospheric radiation ($L_r{}^{\downarrow}$) calculated using the basic model (Equation (9)), LWR of the first term of the right-hand side of Equation (12) ($(1-t_r)$ $\{(1-\phi)$ $L_a{}^{\downarrow}\}$) of the revised model and the second term of the right-hand side of the same equation ($(1-t_r)\phi L_{strc}{}^{\downarrow}$).

The accuracy of the calculated LWR was determined by comparing it with the measured LWR and calculating the root mean square error (RMSE) (Equation (17)).

$$RMSE=\sqrt{\frac{1}{n}\sum_{i=1}^{n}(y_i-\hat{y}_i)^2} \tag{17}$$

where

y_i = calculated value, and

$\hat{y}_i$ = measured value.

The basic model had a RMSE of 39.5 W m^{-2}, whereas the revised model had a RMSE of 17.8 W m^{-2}. The revised model estimates the LWR more accurately than the basic model does.

Amount of cloud affects the accuracy of the LWR estimate. When the difference between total cloud amount (C) and lower cloud amount (C_L) is large, such as on February 1, 7 and 14 (Fig. 4(b)), the error of LWR calculated by the basic model is large (Fig. 4 (a)) and the error of LWR calculated by the revised model is smaller; an improvement by the basic model

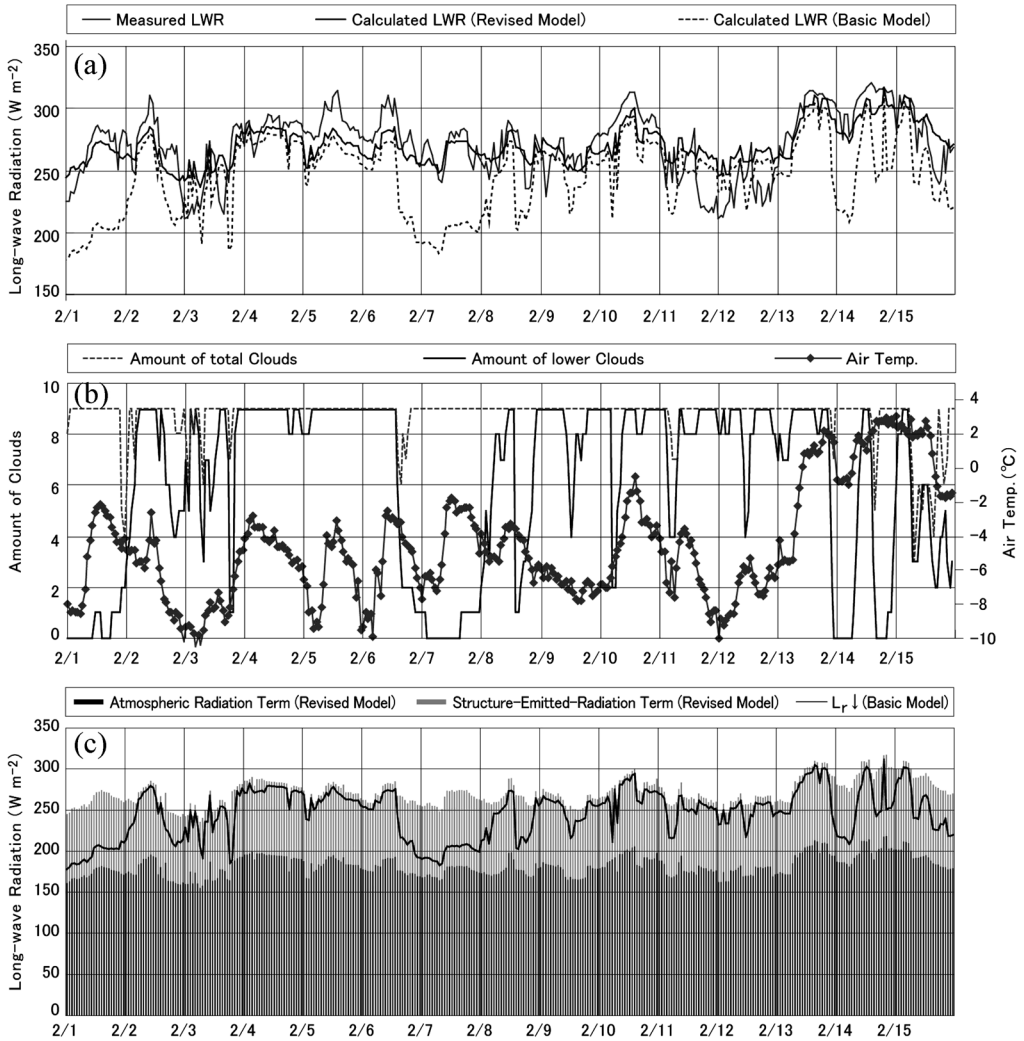

Fig. 4 LWR estimate and measured data. (a) measured and calculated LWR, (b) amount of total and lower clouds, and air temperature and (c) the long-wave radiant quantities calculated by Equation (9) of the basic model, and the atmospheric radiation term ($(1-t_r)\{(1-\phi)L_a^{\downarrow}\}$) and the structure-emitted-radiation term ($(1-t_r)\phi L_{strc}^{\downarrow}$) in Equation (12) of the revised model.

over the revised model can be seen. When both C and C_L are large, such as on February 4 and 5 (Fig. 4 (b)), the accuracy of the calculated LWR is generally high (Fig. 4 (a)).

The LWR calculated by the revised model showed underestimation in daytime, such as on February 5, 6 and 10 (Fig. 4 (a)) and overestimation from the afternoon of February 11 to the end of Feburary 12. Underestimation of LWR by the revised model coincides with high daytime air temperature, and overestimation with relatively lower air temperature (Fig. 4 (b)). The underestimation and overestimation of LWR for the revised model might have occurred as a result of using air temperature in place of surface temperature of structures along the roadway. When the air temperature is high in daytime, the surface temperatures of the structures along the roadway might be higher than the air temperature, from incom-

ing solar radiation; whereas, when the air temperature is low, mainly during nighttime, the surface temperatures of the structures along the roadway might be lower than the air temperature, possibly as a result of radiative cooling at the surcture surface.

The term of atmospheric radiation and outgoing radiation from sturctures in the revised model is shown in Fig. 4 (c). Under the winter weather conditions of Sapporo, LWR emitted by structures ($L_{\mathrm{strc}}{}^{\downarrow}$) is greater than the atmospheric radiation ($L_{\mathrm{a}}{}^{\downarrow}$). To improve the RST estimate, it is important to evaluate the long-wave radiant quantities from structures more accurately.

5.2 Accuracy of road surface temperature estimates

Figure 5 shows the measured RST, along with the RSTs calculated by the basic and the revised models. Calculation was performed for every 10 minutes. Air temperature, wind velocity, and RST were measured every 10 minutes, and other values were obtained from the meteorological observatory every 1 hour. In Fig. 5, the calculated and measured RST is plotted for every hour from the first to the tenth day of each month, from December 2005 to March 2006.

Table 2 shows the monthly average of RMSE. The daytime period is 6: 00 A.M. to 6: 00 P.M. and the nighttime period is 6: 00 P.M. to 6: 00 A.M. As shown in Table 2, the improvement in accuracy of the revised model over the basic model is obvious. The RMSE of the revised model shows an improvement of 1.5 degrees Celsius in daytime, 1.7 degrees Celsius in nighttime and of 1.6 degrees Celsius for all day. Relatively large errors are seen in February and March. This is due to the large fluctuation in measured RST after the end of January (Fig. 5).

Next we explain how the improvement in the estimation accuracy of long-wave radiant quantities affects the accuracy of RST estimation. Figure 6 (a) shows the measured RST and those calculated by the basic and the revised models. Figure 6 (b) indicates the difference between the measured and the calculated long-wave radiant quantities. Figure 6 (c) shows the amount of cloud and solar radiation. The examination was done for the period from February 1 to 2, when measured RST did not show a large fluctuation. As shown in Fig. 6 (a), the basic and the revised models both have a tendency to underestimate the RST; however, the RST estimation accuracy is significantly improved in the revised model: The mean error of RST estimated for the analyzed period is 3.2 degrees Celsius for the basic model and only 1.4 degrees Celsius for the revised model.

The basic model underestimates long-wave radiant quantities relative to the measured values (Fig. 6 (b)). The maximum error is around 80 W m^{-2}. The revised model overestimates the long-wave radiant quantities by 42 W m^{-2} relative to the basic model, and the error relative to the measured values is nearly 30 W m^{-2} at most. The revised model is improved with regard to accuracy in estimating long-wave radiant quantities. In addition, the revised model underestimates the RST relative to that measured from 0 : 00 to 6 : 00 A.M. on February 1. In this period, the error of long-wave radiant quantities for the revised model is -15 to -30 W m^{-2}, i.e., the revised model overestimates long-wave radiant quantities by 15 to 30 W m^{-2} relative to the measured values. This might have caused the overestimation in RST.

Here we discuss the dependency of the RST estimate on solar radiation. The daytime RST was underestimated by the revised model, de spite the improved estimation accuracy of long-wave radiant quantities. When there is incident solar radiation, the calculated RST errors

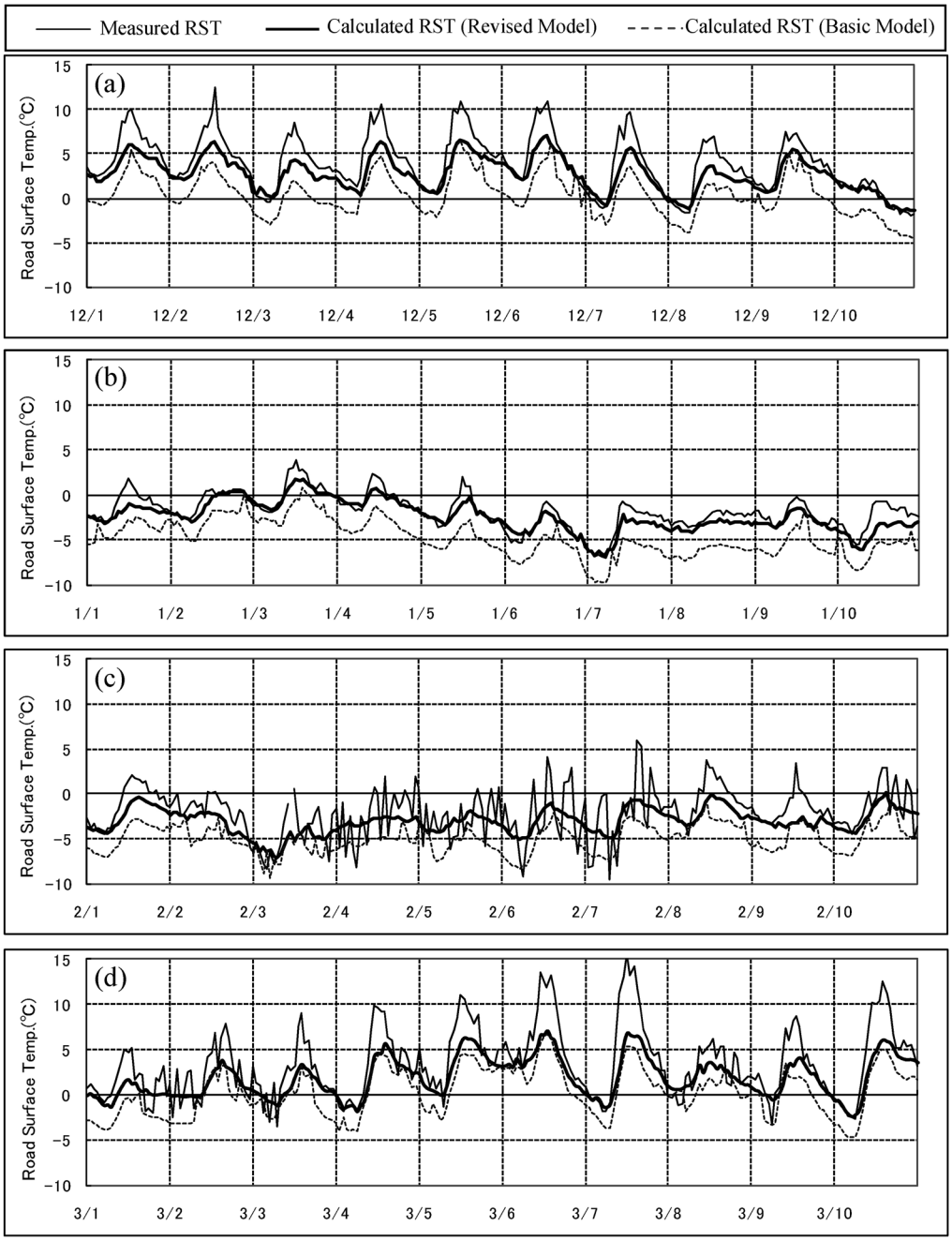

Fig. 5 Estimated and measured RST. (a) December 1 to 10, (b) January 1 to 10, (c) February 1 to 10 and (d) March 1 to 10.

increased with the amount of solar radiation. This was consistent through the analyzed period. The example is shown in Fig. 7. To improve the estimation accuracy of RST, it is necessary to improve the estimation accuracy of the amount of solar radiation.

In the revised model, the rate of radiation shielding (ϕ) is a fixed value. It varies with the

Table 2 RMSE of RST calculation.

	All Day		Daytime (6:00A.M. to 6:00P.M.)		Nighttime (6:00P.M. to 6:00 A.M.)	
	Basic Model	Revised Model	Basic Model	Revised Model	Basic Model	Revised Model
December	3.2	1.3	3.5	1.7	2.8	0.7
January	3.4	1.5	3.7	1.9	3.1	1.2
February	3.8	2.7	4.5	3.4	3.1	1.8
March	3.8	2.7	4.6	3.6	2.8	1.3
Average	3.5	1.9	3.9	2.4	3.0	1.3

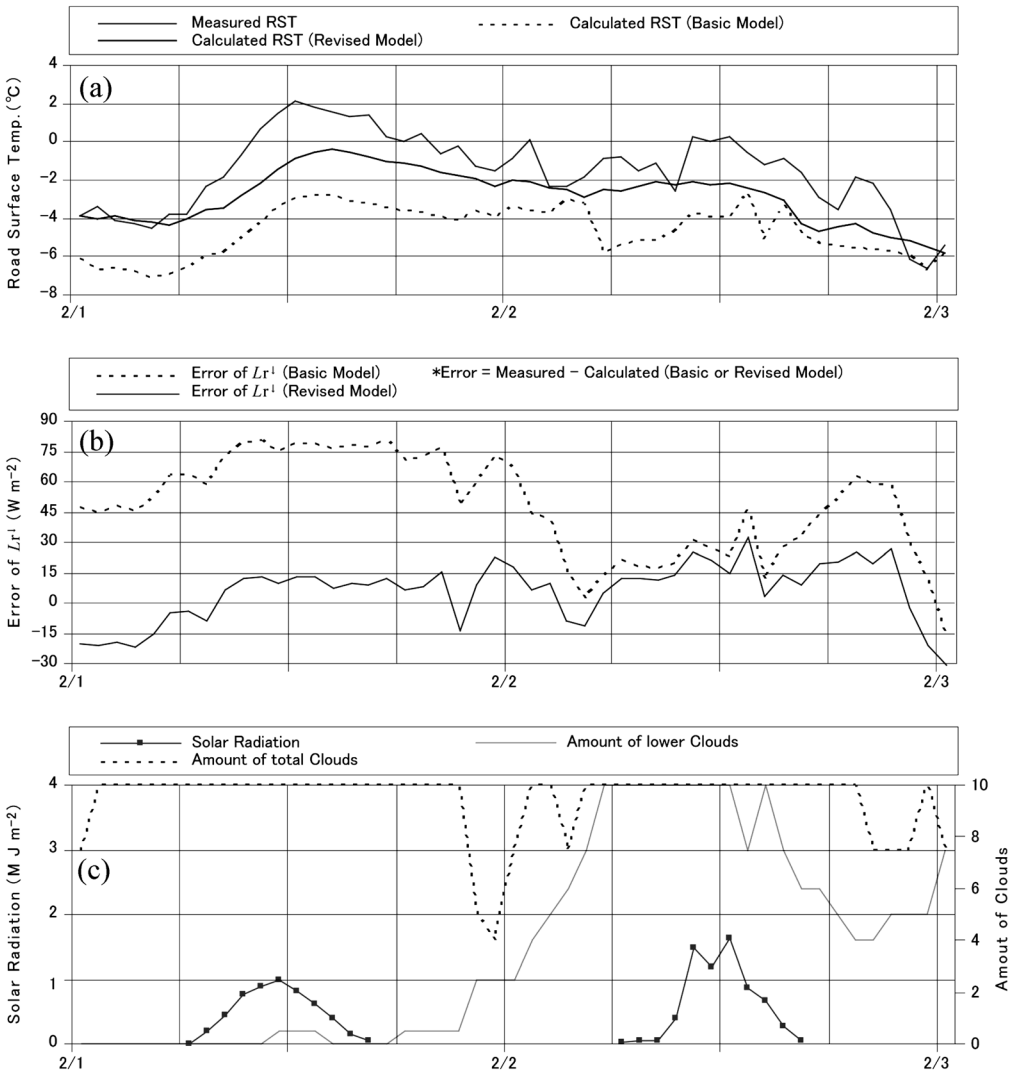

Fig. 6 RST estimate and measured data. (a) measured RST and those calculated by the basic and the revised models, (b) difference between measured and calculated long-wave radiant quantities and (c) amount of clouds and solar radiation.

position of the sun and the shape of surrounding structures. The constant ϕ applied for the revised model could be greater than the actual rate of radiation shielding, depending on the position of the sun. As a result, RST may be underestimated relative to measured RST.

6. Conclusions

We have assumed that structures along the roadway are the primary cause of error in the RST estimated by the basic model, so the shielding effect of structures along the roadway was taken into consideration in the revised model.

The model has been expanded and improved to account for blockage of solar and atmos pheric radiation and for LWR emitted by structures along the roadway. In the revised model, the RMSE of RST calculation was 1.9 degrees Celsius for the whole day, 2.4 degrees Celsius in the daytime and 1.3 degrees Celsius in the nighttime: The accuracy was improved by 1.6 degrees Celsius for the whole day, 1.5 degrees Celsius in the daytime and 1.6 degrees Celsius in the nighttime. This technique is effective in large cities with heavy traffic and many structures along roadways, such as Sapporo.

RST is, in turn, a very important element of winter maintenance decision-making, especially when temperatures are near the freezing point and the probability of road icing is uncertain. For this reason, further work is required to improve the accuracy of the RST model.

Based on the study results, the following suggestions to improve the accuracy of RST estimation are made.

(1) *Improvement in estimation accuracy of long-wave radiant quantities*

The estimation accuracy of long-wave radiant quantities was improved significantly by considering the effect of structures along the roadway in the revised model. It is thought that the improvement in the estimation accuracy of long-wave radiant quantities increased the accuracy of RST estimation. In this study, the structure's surface temperature is assumed to be equal to the air temperature. However, the actual structure surface temperature might be higher or lower than the air temperature. Therefore, to improve the estimation accuracy of long-wave radiant quantities, it is necessary to measure both the structure's surface temperature and the air temperature, and to verify its relationship.

(2) *Improvement in estimation accuracy of amount of solar radiation*

When there was sunlight, the accuracy of RST estimation was too low, and this resulted in RST underestimation. There is a possibility that the revised model underestimates the quantity of solar radiation. In the revised model, the screening factor of solar radiation is made into a steady value. In fact, the screening factor varies with the position of the sun. This might cause the solar radiation to be

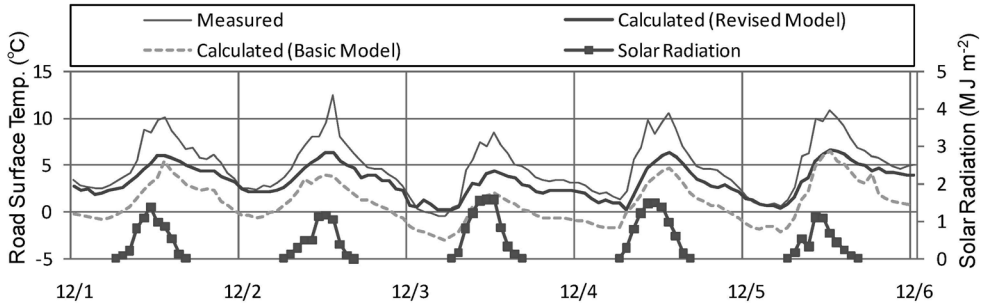

Fig. 7 Calculated RST, measured RST and solar radiation (December 1 to 5, 2005).

underestimated. Therefore, we need to improve the model such that it is able to account for time-dependent differences in the screening factor by measuring both the amount of solar radiation and the position of the sun at the study point.

References

Bentz, D.P. and Dale, P., 2000: A computer model to predict the surface temperature and time-of-wetness of concrete pavements and bridge decks. National Institute of Standards and Technology. NISTIR 6551.

Brown, B.G. and Murphy, A.H., 1996: Improving Forecasting performance by combining forecasts: The example of road-surface temperature forecasts. Meteorological Applications, **3**, 3, 257–265.

Chapman, L. and Thornes, J.E., 2005: The influence of traffic on road surface temperatures: Implication for thermal mapping studies. Statistical Meteorological Applications, **12**, 371–380.

Chapman, L., Thornes, J.E. and Bradley, A.V., 2001: Modeling of road surface temperatures from a geographical parameter database. Statistical Meteorological Applications, **8**, 409–436.

Civil Engineering Research Institute, 2005: Study report on snow and ice control techniques. Civil Engineering Research Institute.

Erbs, D.G., Klein, S.A. and Duffie, J.A., 1982: Estimation of the diffuse radiation fraction for hourly daily and monthly-average global radiation. Solar Energy, **28**, 293–302.

Ishikawa, N., Narita, H. and Kajiya, Y., 1999: Contributions of heat from traffic vehicles to snow melting on roads. Transportation Research Record, **1672**, 28–33.

Johnson, G.T., Oke, T.R., Lyins, T.J, Steyn, D.G., Watson, J.D. and Voogt, J.A., 1991. Simulation of surface urban heat islands under "Ideal" conditions at night, Part2: Diagnosis of causation. Boundary-Layer Meteorology, **56**, 339–358.

Kondo, J., 1994: Metrology of water environment: Water-and heat-balance of land surface, Tokyo. Asakura Publishing, ISBN4-254-16110-7.

Mahoney, W.P. and Wagoner, R.A., 2005: Surface transportation weather forecasting and observations: Assessment of capabilities and future trends. Proceedings of the 2005 Mid-Continent Transportation Research Symposium, ISBN 978-0-9652310-8-4.

Narita, K., 2001: Moving observation of downward long-wave radiation in and around Tokyo. Papers on Environmental Information Science, **15**, 249–254.

Oke, T.R., 1978: Boundary layer climates. Methuen & Co., Ltd.

Prusa, J.M., Segal, M., Temeyer, B.R., Gallus Jr., W.A. and Takle, E.S., 2002: Conceptual and scaling evaluation of vehicle traffic thermal effects on snow/ice-covered roads. Journal of Applied Meteorology, **41**, 1225–1240.

Rayer, P.J., 1987: The meteorological office forecast road surface temperature model. The Meteorological Magazine, **116**, 180–191.

Seki, H., Ishida, H., Nishitani, N. and Kitagawa, K., 2006: Development of mathematical model to predict road surface temperature with heat conduction analysis and its validity. 18th Yuki-Mirai Research Presentation, CD-ROM.

Shao, J. and Lister, P.J., 1996: An automated nowcasting model of road surface temperature and state for winter road maintenance. Journal of Applied Meteorology, **35**, 1352–1361.

Takahashi, N., Tokunaga, R.A., Asano, M. and Ishikawa, N., 2006: Toward strategic snow and ice control on roads: Developing a method for surface-icing forecast with applying a heat balance model. Transportation Research Board 85th Annual Meeting, CD-ROM.

Takle, E.S. and Hansen, Jr., S.T., 1990: Development and validation of an expert system for forecasting frost on bridges and roadways. Preprints, Sixth International Conference on Interactive Information and Processing Systems for Meteorology, Oceanography and Hydrology, Anaheim, California, 197–200.

Thornes, J.E. and Shao, J., 1991: Spectral analysis and sensitivity tests for a numerical road surface temperature prediction model. The Meteorological Magazine, **120**, 1428, 117–120.

Watanabe, H., Fujimoto, A. and Fukuhara, T., 2005: Modeling of heat supply to pavement from vehicle. Proceedings of 2005 Cold Region Technology Conference, 195–200.

沿道構造物の影響を考慮した路面温度予測モデル

高橋尚人[1)]，徳永 A. ロベルト[1)]，佐藤隆光[2)]，石川信敬[3)]

[1)]（独）土木研究所寒地土木研究所　〒062-8602 札幌市豊平区平岸 1 条 3 丁目
[2)]（財）日本気象協会　〒170-6055 東京都豊島区東池袋 3-1-1
[3)] 北海道大学低温科学研究所　〒060-0819 札幌市北区北 19 条西 8 丁目

要　旨

冬期路面管理をより適確に行う上で，路面温度予測や路面状態予測は重要な技術である．筆者らは，熱収支法を用い，走行車両の影響を考慮した路面温度モデルの構築に取り組んでいる．当該モデルによる計算結果は路面温度変化の傾向を捉えているが，路面温度を実測より低めに計算する傾向にあった．路面温度が低めに計算されるのは，沿道の構造物の影響を見込んでいないことが原因と考え，当該モデルに沿道構造物による遮蔽と沿道構造物の長波放射を考慮する改良を加えた．更に，観測地点に長波放射計を設置して長波放射量の観測を行い，改良モデルの有効性を検証した．結果，長波放射量の計算値の二乗平均平方根誤差（RMSE）は 17.8 W m^{-2} になった．路面温度の推定誤差は，全日で 1.9℃，昼間 2.4℃，夜間 1.3℃となった．改良前と比べ，全日で 1.6℃，昼間 1.5℃，夜間 1.7℃ 精度が向上した．

キーワード：路面温度，熱収支法，沿道構造物，長波放射

（2009 年 1 月 31 日受付，2009 年 8 月 10 日改稿受付，2010 年 10 月 5 日最終改稿受付，
2010 年 10 月 12 日受理，討論期限 2011 年 5 月 15 日）